

**GT2005-68927**

## **OVERVIEW OF CREEP STRENGTH AND OXIDATION OF HEAT-RESISTANT ALLOY SHEETS AND FOILS FOR COMPACT HEAT-EXCHANGERS**

**Philip J. Maziasz, John P. Shingledecker, Bruce A. Pint, Neal D. Evans,  
Yukinori Yamamoto, Karren More and Edgar Lara-Curzio**

Oak Ridge National Laboratory  
Metals and Ceramics Division

Oak Ridge, TN 37831-6115

Phone: (865) 574-5082, e-mail: [maziaszpj@ornl.gov](mailto:maziaszpj@ornl.gov)

### **ABSTRACT**

The Oak Ridge National Laboratory (ORNL) has been involved in research and development related to improved performance of recuperators for industrial gas turbines since about 1996, and in improving recuperators for advanced microturbines since 2000. Recuperators are compact, high efficiency heat-exchangers that improve the efficiency of smaller gas turbines and microturbines. Recuperators were traditionally made from 347 stainless steel and operated below or close to 650°C, but today are being designed for reliable operation above 700°C. The Department of Energy (DOE) sponsored programs at ORNL have helped defined the failure mechanisms in stainless steel foils, including creep due to fine grain size, accelerated oxidation due to moisture in the hot exhaust gas, and loss of ductility due to aging. ORNL has also been involved in selecting and characterizing commercial heat-resistant stainless alloys, like HR120 or the new AL20-25+Nb, that should offer dramatically improved recuperator capability and performance at a reasonable cost. This paper summarizes research on sheets and foils of such alloys over the last few years, and suggests the next likely stages for manufacturing recuperators with upgraded performance for the next generation of larger 200-250 kW advanced microturbines.

### **INTRODUCTION**

Microturbines are ultraclean, relatively quiet, and fuel flexible, and are attractive for distributed generation (DG), combined heat and power (CHP), and possibly combined cycle (microturbine-fuel cell) applications. DG can immediately remedy some of the power transmission grid problems and deficiencies that were magnified by the Blackout of 2003 in the Midwestern and the Northeastern U.S.[1]. Microturbines can

also play an important role in various homeland security strategies in the U.S. by removing critical facilities, like hospitals and water treatment plants and infrastructure, from dependence on the electric grid [1,2]. Recuperators are the compact heat exchangers necessary for high-efficiency, advanced microturbines; however, recuperators are also a costly and challenging component of such systems that limit maximum operating temperature and lifetime [3-5]. Recuperators for industrial turbines and microturbines have traditionally been made from 347 stainless steel, but problems with performance and durability are becoming evident for such steels as temperatures approach or exceed 675-700°C, particularly in moist air. Economic and efficiency advantages have pushed microturbine engine sizes up from 30-70 kW to 200-250 kW, for both stand-alone power generation and CHP applications. If microturbines are used to generate power during peak demand, then cycling will further challenge the recuperator with thermal shock during rapid heat-up. Durable, reliable recuperators (and packaging or ducting) are critical components for any attractive microturbine systems.

### **RECUPERATOR DEVELOPMENT OVER THE LAST DECADE**

Today, there are two main types of recuperator used on commercial microturbines in the U.S. Both are compact, counterflow recuperators with high effectiveness, and both are designed for high quality mass manufacturing at a reasonable cost [4]. One type is the primary surface recuperator (PSR), designed by Solar Turbines and Caterpillar; it consists of welded air cells made from folded foils, and is used in several different kinds of final geometries [3-6]. Rectangular PSR air cell stacks positioned horizontally above the engine have been employed in various Solar Turbines industrial gas turbines, in

Honeywell 75kW microturbines, and most recently, in the new Mercury 50 4.6 MW gas turbine engine [7]. The Capstone Turbines microturbine systems (30kW, 60kW, and new 200kW units) all have used specially-designed annular assemblies of the PSR air cells, which surround the turbine [8]. The other type is the brazed plate and fin recuperator (BPFR), which includes (a) the completely-brazed, vertical stack developed by Toyo [5], and (b) the uniquely-designed air cells of folded foils brazed to sheet-plates which are also stacked vertically and were developed by Ingersoll Rand for their PowerWorks 70 kW, and new 250 kW, microturbines [9]. The Ingersoll Rand BPFR made from foils and sheets of alloy 625 is also employed on the Rolls Royce WR21 advanced cycle gas turbine designed for naval marine applications [10]. Another type of primary surface recuperator is the spirally-wrapped recuperator, manufactured by continuously spooling foils or sheets [5], with different designs and sizes being developed by Rolls Royce [11] and by Acte, S.A. [12].

Development of durable and reliable recuperator technology has paralleled and been pushed by the introduction of commercial microturbines in 1996-1997, in conjunction with the initial and continuing phases of a collaboration by Southern California Edison, U.S. Department of Energy (DOE), and others to study the installation, operation and maintenance of microturbines to promote distributed power generation [13,14]. Another driver for the development of higher temperature recuperators came from the DOE Advanced Microturbine Program in 2000 [15], which included the ambitious goal to design and build microturbines with efficiencies of 40% or more. Prior to 2000, recuperators were made almost exclusively from 347 stainless steel (Fig. 1) [5,16], and generally performed well at temperatures below 650°C (1200°F). More recent research has highlighted the problems that can limit the performance of 347 stainless steel at 675-700°C (about 1250-1300°F) and above, particularly the accelerated attack (AA) caused by moisture enhanced oxidation at these conditions (Fig. 2) [17,18]. Larger microturbines with higher efficiencies will also operate with higher temperatures and pressures in the recuperator. Focused research on the DOE Advanced Microturbines Program over the last several years has defined and addressed the needs for better metal foils and sheets that can withstand prolonged use at higher temperatures, but which also still remain affordable for recuperator applications.

## **SUMMARY OF CHALLENGES TO METAL SHEET/FOIL RECUPERATORS**

The first challenge is, of course, manufacturing the desired components, but by far the greatest challenge is long-term operation at elevated temperatures without failure. While the minimum need for recuperators is to survive until scheduled maintenance intervals (5000 to 10,000 h), the desired lifetime is the same as that of the overall microturbine system, which can range from 40,000 to 80,000 h [13,15]. Both PSR and BPFR air cells are made using high-quality, automated and/or continuous manufacturing processes that produce consistent results, and each air cell is pressure checked at room temperature to ensure no leakage [8,9].

In service, several metallurgical effects of high-temperature exposure can degrade recuperator performance prior to the cracking that causes leakage of pressurized air into the exhaust, or the severe deformation that reduces effectiveness. These effects include oxidation, creep, fatigue, and aging-

induced precipitation in the matrix and along grain boundaries of the alloy. For 347 stainless steel, such effects are not significant at 1100-1200°F, become concerns at 1200-1250°F, and can be severe at 1300°F and above. Creep can close the exhaust gas passages of a PSR to restrict gas flow, and the heavy ferrous oxide growth on the surfaces of foils associated with severe AA can reduce thermal conductivity and heat transfer. Oxidation resistance is mainly a function of alloy composition (Cr and Ni contents [19]), but oxidation, creep and aging behavior can all also be affected by metallurgical processing parameters (ie. grain size, solution annealing (SA) temperature, dispersion and abundance of various precipitate phases).

The significant differences in manufacturing processes between PSR and BPFR air cells may also affect how they behave, particularly for service above 1300°F. The PSR air cells are made from folded foils of 347 stainless steel that are 0.003 to 0.005 in. thick, and are welded to similar steel wire or bar (321 or 347 steel) to form the seal at the end. Folding produces from 5-15% cold strain in the foil, depending on the location along the fold. However, the ends of the foil near the weld are crushed flat prior to welding, so they may be cold-worked 30% or more. Relative to SA material (which is usually tested to produce properties data), 20-25% cold-working can enhance the formation of deleterious intermetallic phases ( $\sigma$ , Laves) during aging, and would certainly cause recrystallization of the original grain structure into a new fine-grained microstructure, with details that are very sensitive to minor or impurity alloying elements in austenitic stainless steels [20-22]. Moreover, 5-15% cold work can cause either accelerated or retarded creep-rates [20-22]. By contrast, BPFR air cells are welded to seal the ends and then brazed, which removes all prior cold deformation and restores all the materials in the air cell to a SA condition. However, the braze joint and its effects on the bonded stainless steel sheets and foils are an additional and unique factor that needs to be considered for this kind of recuperator. To date, there are no systematic studies or data to address all of these concerns, but data should be accumulated as ongoing studies of turbine-exposed or failed air cells continue, particularly the studies from the ORNL Recuperator Test Facility [23].

## **SELECTION AND EVALUATION OF ADVANCED ALLOYS FOR RECUPERATORS WITH HIGHER-TEMPERATURE CAPABILITY**

### **Creep-Rupture Testing of Advanced Alloys**

Advanced alloy sheets and foils with higher-temperature capability and more reliability than type 347 stainless steel (Fe-18Cr-10Ni) above 700°C are heat- and corrosion-resistant alloys with more Cr and more Ni, plus various other alloying elements added for more strength. However, these elements, particularly Ni, make better alloys more expensive, so that higher cost must also be balanced with improved performance. Relative to the same alloys made as coarse-grained plate or tubing, fine-grained foils tend to be much weaker in creep; therefore, there is no guarantee that alloy rankings from strongest to weakest will be the same for both foil and plate products. ORNL worked with Solar Turbines and Allegheny-Ludlum in 1996-1999 to define creep properties of foils of type 347 stainless steel, and lab-scale experiments led to modified processing parameters for improved creep-rupture resistance [22,24]. In 2002-2003, ORNL and Allegheny Ludlum engaged

in a follow-up commercial-scale 347 steel foil and sheet processing effort [25-27], and produced AL347HP™ with more creep-resistance, which is now commercially available [27]. However, improved creep strength and rupture resistance for foils and sheets of 347 steel still does not solve the inherent oxidation and AA problem; oxidation data in air with 10% H<sub>2</sub>O shows severe AA after only about 1000 h at 650°C [25,26,28].

Since about 2000, there have been several broader studies considering the properties of foils made from a range of heat-resistant and corrosion resistant alloys for microturbine applications [16,23,25,26,28-32]. These alloys can be divided into two groups, one for alloys that can be used from 650°C to up to 800°C, and the other for use at 800°C and above. Many of these alloys are also considered and used for many other high-temperature applications of thicker, larger components, including power boiler and turbine applications [33-36]. For temperatures above 800°C, Ni-based alloys with aluminum, for example HR214, or the Fe-based oxide dispersion-strengthened (ODS) Plansee alloy, PM2000, have both the strength and oxidation resistance as sheets and foils to be used for recuperators. However, fabricating and manufacturing recuperator air cells or components from such alloys may be more difficult, and their cost is at least ten times that of 347 stainless steel. There are several commercial or near-commercial alloys that show good strength and oxidation resistance at 650-750°C, including alloy 625 (Ni-22Cr-9Mo-3.5Nb), HR120 (Fe-25Cr-35Ni – Mo,Nb,N) and the new AL20-25+Nb (Fe-20Cr-25Ni – Mo,Nb,N), which are 2-4 times more expensive than 347 steel. ORNL efforts in the last few years have focused on testing and evaluating commercial sheets and foils of these particular alloys, because of their interest to recuperator manufacturers.

Results of creep testing of recent commercial sheets and foils obtained from commercial materials producers or from recuperator manufacturers, creep-rupture tested at 750°C and 100 MPa, are shown in Fig. 3. PM2000 sheet showed virtually no creep (even at 120 MPa), and alloy 625 showed very little after 7000-8000h (both tests are ongoing). Previous results for alloy 625 foil with lab-scale processing at ORNL indicated rupture after only about 4500h at the same creep conditions, so that the commercial sheet is much stronger. Both alloy 625 and PM2000 would have advantages for recuperators in which strain limits, rather than rupture, define lifetime. Alloy 625 is being used for the PSR for the Solar Turbines Mercury 50 industrial turbine engine [7], and for the Ingersoll-Rand BPFR used with the Rolls-Royce WR-21 marine turbine engine [10]. Given the combination of cost and creep resistance, alloy 625 is clearly the most cost effective at about 3.5-4 times the cost of 347 steel [9,16]. Foils of HR120 and HR230 (0.003-0.004 in. thick) show much less creep resistance than alloy 625, but are still about ten times better than 347 steel.

The effects of grain size/processing on creep resistance at these conditions are shown for HR230 in Fig. 4 and HR120 in Fig. 5. Thicker products (boiler-tubing, plate) of HR230 showed much more creep resistance than foils [36], indicating that these foils have a grain size below the critical grain size for creep resistance in this alloy (typically 10-20 μm grain size). Processing and microstructural behavior during aging determine such creep behavior, with foils usually being exposed to somewhat lower processing temperatures, and much shorter processing times than plate or tubing products. Given the tubing behavior, it is unlikely that sheet of HR230 would perform

as well as alloy 625, and at 8-9 times the cost of 347 steel, HR230 is not a cost-effective choice.

By contrast, the creep-rupture resistance of HR120 is similar for foil and bar products (Fig. 5), indicating much less sensitivity to grain size/processing than HR230. However, previous ORNL data on a similar foil showed 2-3 times better creep resistance for the same test conditions [25,32], so that there is clearly a need for more data to better define the typical creep resistance of such foils and their microstructural characteristics. It is likely that HR120 sheet would have similar creep resistance as foil, and at about 3.5 times the cost of 347 steel, this also represents a cost-effective performance upgrade, particularly considering its excellent oxidation resistance.

Creep-rupture testing on this group of alloys was also performed at 704°C (1300°F) and 150 MPa, because most near-term microturbine recuperators would benefit from reliable materials that can be used at or slightly above this temperature; data are shown in Fig. 6. Alloy 625 sheet was very creep-resistant (test is ongoing), while 347 steel foil was very weak. The two foils of HR120 alloy behaved differently, with one being only slightly weaker at 704°C, and the other being several times weaker than the same foils tested at 750°C [25,26].

In 2003-2004, Allegheny Ludlum introduced a new high temperature alloy, AL20-25+Nb, which was developed together with Solar Turbines for foil recuperator applications [6]. This alloy is another in a group of improved alloys based on the austenitic stainless alloy composition of Fe-20Cr-25Ni developed during the 1980's, which includes British work on that alloy for high-temperature gas-cooled fission reactors, Nippon Steel Corp.'s NF709 and Sandvik's 12R72HV, for fossil energy boiler tubing with more corrosion resistance and creep strength than 17-14CuMo and 347H stainless steels [34, 37-39]. ORNL made some lab-scale foils, rolled from slit and flattened NF709 boiler tubing, for creep and oxidation testing in 2001-2003 [25,26,28]. Based on these preliminary results, interest from the microturbine recuperator manufacturers, and potential for pricing inbetween the cost of 347 steel and alloy 625, ORNL and Allegheny defined a joint project in 2004 to expand commercial foil development for microturbine recuperator manufacturers. Phase I of this project has produced 10 and 15 mil sheets and 4, 5 and 8 mil foils in commercial quantities suitable for manufacturing trials of PSR and BPFR recuperator aircells. ORNL is currently performing creep-testing and microstructural analyses. Creep rupture data for a foil of AL20-25+Nb at 704°C are also shown in Fig. 6. The creep resistance of AL20-25+Nb was only slightly less than that of HR120 (particularly below 5% strain), and several times better than standard 347 steel, with excellent rupture ductility. Based on these initial data, ORNL and Allegheny-Ludlum are now defining processing changes that can improve the creep-resistance (similar to the previous joint project on 347 steel [25-27]), and then will produce limited quantities of selected sheets and foils in a Phase II effort of commercial processing.

These advanced alloys, particularly HR120 and AL20-25+Nb, are expected to provide microturbine recuperators with all of the fabrication benefits of 347 steel (easy folding, welding and brazing), and still provide performance and durability improvements, even with higher recuperator temperatures, cyclic operation or alternative, more corrosive opportunity fuels (flare gas, land-fill gas, biofuels, etc.).

### **Microstructural Analysis of Creep-Tested Foils**

Microstructural analysis of the gage portions of creep-ruptured foil specimens tested at 704 or 750°C has included scanning and analytical electron microscopy (SEM and AEM) to characterize the microstructural changes and identify precipitate phases forming during creep. Creep data on these alloys, including 347 steel, and alloys HR120, NF709 and 625, have been published previously [25,26]. Figure 7a shows the formation of Fe-Cr  $\sigma$ -phase at grain boundary triple points in standard 347 steel (having a very fine, 2-5  $\mu\text{m}$  grain size) after only 51.4h creep at 704°C. Coarser-grained (>20  $\mu\text{m}$ ) alloy 625 creep-tested at 750°C for 4510h exhibited a stable dispersion of Si-Mo-Cr-Ni  $\text{M}_6\text{C}$  particles along the grain boundaries, and dense lath/subgrain boundary structure within each grain (Fig. 7b). The grains in alloy 625 showed no dislocation networks and no fine  $\gamma'$  precipitation. Apparently the fine laths and intergranular precipitation helped to provide the creep-strength observed in alloy 625.

The NF709 and HR120 austenitic stainless alloys developed similar grain boundary structures during creep, but exhibited somewhat different intragranular precipitate structures, as shown in Fig. 8. The NF709 showed a finer grain structure (10-15  $\mu\text{m}$ ), a uniform dispersion of mainly Si-Mo-Cr-Ni  $\text{M}_6\text{C}$  and some Cr-rich  $\text{M}_{23}\text{C}_6$  particles along the grain boundaries, and little or no coarse intragranular precipitation after 5015h of creep. By comparison, the HR120 had a coarser grain structure (30-40  $\mu\text{m}$ ), and copious precipitation of  $\text{M}_{23}\text{C}_6$  along the grain boundaries and inside the grains. Higher magnification AEM showed that both NF709 and HR120 contain fine dispersions of NbC precipitates within the grains that formed during creep and pinned the dislocation networks. The stable carbide strengthening of grain boundaries and matrix provides the creep resistance for both of these alloys.

### **Screening in the ORNL Recuperator Test Facility**

Commercial foils and sheets of advanced alloys evaluated by laboratory creep and oxidation tests at ORNL are also being evaluated in an actual microturbine exhaust environment in the ORNL Recuperator Test Facility, based on a modified Capstone 60 KW microturbine [23,40]. More comprehensive test data on many different alloys has been presented elsewhere [23], and data directly comparing standard 347 steel and HR120 alloy foils, as well as other alloys, are presented in another paper at this conference [41]. Actual recuperator applications involve much lower stresses than the high-stress creep-rupture tests described above, but do include the dynamic interplay of stress, creep and oxidation with water vapor in a flowing, high gas velocity environment. Initial screening tests for 500h clearly show that 347 steel foils degrade rapidly due to moisture-induced AA during oxidation and creep at 700°C and above. Consistent with the relative alloy comparisons in this work, the HR120 alloy has dramatically better performance at 700°C and above. Currently, similar testing of the ORNL modified 347 steels developed earlier [25,26] is in progress, and testing of foils of the new AL20-25+Nb alloy will begin shortly.

### **SUMMARY AND FUTURE WORK**

Alloys 625 and HR120 are commercially available in sheet and foil forms that have significantly better oxidation- and creep-resistance compared to standard commercial 347 steel at 650-750°C. Such property differences should enable enhanced performance and temperature capability of recuperators at

about 3.5-4 times the cost of 347 steel. The new AL20-25+Nb alloy has the potential to offer similar improvements in performance at a lower cost.

### **ACKNOWLEDGEMENTS**

Cooperation of Capstone Turbines, Inc., and Ingersoll-Rand Energy Systems, with the materials research efforts at ORNL is greatly appreciated. Research was sponsored by the U.S. Department of Energy, Assistant Secretary for Energy Efficiency and Renewable Energy, Office of Distributed Energy and Electrical Reliability, under contract DE-AC05-00R22725 with UT-Battelle, LLC.

### **REFERENCES**

1. DG Monitor, Vol. III, issue 5, September/October 2003, Resource Dynamics Corp., Vienna, VA.
2. "Microturbines are Generating Interest," Materials and Components in Fossil Energy Applications, Newsletter No. 143 (Dec. 1, 1999), U.S. DOE and EPRI, published by Oak Ridge National Laboratory, Oak Ridge, TN.
3. Ward, M.E., 1995, "Primary Surface Recuperator Durability and Applications," Report No. TTS006/395, Solar Turbines, Inc., San Diego, CA.
4. McDonald, C.F., 1996, "Heat Recovery Exchanger Technology for Very Small Gas Turbines," *International Journal of Turbo and Jet Engines*, **13**, pp.239-261.
5. McDonald, C.F., 2003, "Recuperator Considerations for Future Higher Efficiency Microturbines," *Applied Thermal Engineering*, **23**, pp. 1463-1487.
6. Rakowski, J.M., Stinner, C.P., Lipschutz, M., and Montague, J.P., 2004, "The Use and Performance of Oxidation and Creep-Resistant Stainless Steels in an Exhaust Gas Primary Surface Recuperator Application," ASME paper GT2004-53917, Am. Soc. Mech. Engin., New York, NY.
7. Stambler, I., "Mercury 50 Rated at 4600 kW and 38.5% Efficiency With 5 ppm NOx," 2004, *Gas Turbine World* (Feb.-Mar.), pp. 12-16.
8. Treece, B., Vessa, P., and McKeirnan, R., 2002, "Microturbine Recuperator Manufacturing and Operating Experience," ASME paper GT-2002-30404, Am. Soc. Mech. Engin., New York, NY.
9. Kesseli, J., Wolf, T., Nash, J., and Freedman, S., 2003, "Micro, Industrial, and Advanced Gas Turbines Employing Recuperators," ASME paper GT2003-38938, Am. Soc. Mech. Engin., New York, NY.
10. Branch, D., 2003, "The WR-21 – From Concept to Reality," in Parsons 2003: Engineering Issues in Turbine Machinery, Power Plants and Renewables, The Institute of Materials, Minerals and Mining, Maney Publishing, London, UK, pp. 1039-1055.
11. Oswald, J.I., Dawson, D.A., and Clawley, L.A., 1999, "A New Durable Gas Turbine Recuperator," ASME paper 99-GT-369, Am. Soc. Mech. Engin., New York, NY.
12. Antoine, H., Prieels, L., 2002, "The ACTE Spiral Recuperator for Gas Turbine Engines," ASME paper GT2002-30405, Am. Soc. Mech. Engin., New York, NY.
13. Hamilton, S.L., 2003, The Handbook of Microturbine Generators, PennWell Corp., Tulsa, OK.
14. Agular, V.D., and Hamilton, S.L., 2004, "The Best Applications for Microturbines," *Cogeneration and On-Site Power Production*, **5**, no. 4 (July-August), pp. 101-106.

15. Advanced Microturbine Systems – Program Plan for Fiscal Years 2000 – 2006, Office of Power Technologies, Office of Energy Efficiency and Renewable Energy, U.S. Department of Energy, Washington, D.C. (March 2000).
16. Maziasz, P.J., and Swindeman, R.W., 2003, "Selecting and Developing Advanced Alloys for Creep-Resistance for Microturbine Recuperator Applications," *Journal of Engineering for Gas Turbines and Power* (ASME), **125**, pp. 310-315.
17. Pint, B.A. and Rakowski, J.M., 2000, "Effects of Water Vapor on the Oxidation Resistance of Stainless Steels," paper 00259 from *Corrosion 2000*, NACE-International, Houston, TX.
18. Pint, B.A., More, K.L., and Tortorelli, P.F., 2002, "The Effect of Water Vapor on Oxidation Performance of Alloys Used in Recuperators," ASME paper GT-2002-30543, Am. Soc. Mech. Engin., New York, NY.
19. Pint, B.A., and Peraldi, R., 2003, "Factors Affecting Corrosion Resistance of Recuperator Alloys," ASME paper GT2003-38692 Am. Soc. Mech. Engin., New York, NY.
20. Maziasz, P.J., 1986, "Microstructural Stability and Control for Improved Irradiation Resistance and for High-Temperature Strength of Austenitic Stainless Steels," in MiCon 86: Optimization of Processing, Properties and Service Performance Through Microstructural Control, ASTM-STP-979, ASTM, Philadelphia, PA, pp. 116-161.
21. Maziasz, P.J. and Swindeman, R.W., 1987, "Modified 14Cr-16Ni Stainless Steels With Improved Creep Resistance at 700°C Due to Tailored Precipitate Microstructure," in *Advances in Materials Technology for Fossil Power Plants*, ASM-International, Materials Park, OH, pp. 283-290.
22. Maziasz, P.J., et al, 1999, "Improved Creep-Resistance of Austenitic Stainless Steel for Compact Gas Turbine Recuperators," *Materials at High Temperatures*, **16**(4), pp. 207-212.
23. Lara-Curzio, E., Trejo, R., More, K.L., Maziasz, P.J., and Pint, B.A., 2004, "Screening and Evaluation of Materials for Microturbine Recuperators," ASME paper GT2004-54254, Am. Soc. Mech. Engin., New York, NY.
24. Swindeman, R.W., Maziasz, P.J., Pint, B.A., Montague, J.P., and Fitzpatrick, M, 1996, Evaluation of Stainless Steels for Primary Surface Recuperator Applications, Oak Ridge National Laboratory Report C/ORNL96-0453, Oak Ridge, TN.
25. Maziasz, P.J., Swindeman, R.W., Shingledecker, J.P., More, K.L., Pint, B.A., Lara-Curzio, E., and Evans, N.D., 2003, "Improving High Temperature Performance of Austenitic Stainless Steels for Advanced Microturbine Recuperators," in Parsons 2003: Engineering Issues in Turbine Machinery, Power Plants and Renewables, The Institute of Materials, Minerals and Mining, Maney Publishing, London, UK, pp. 1057-1073.
26. Maziasz, P.J., Pint, B.A., Shingledecker, J.P., More, K.L., Evans, D.E., and Lara-Curzio, E., 2004, "Austenitic Stainless Steels and Alloys With Improved High-Temperature Performance for Advanced Microturbine Applications," ASME paper GT2004-54239, Am. Soc. Mech. Engin., New York, NY.
27. Stinner, C., "Processing to Improve Creep and Stress Rupture Properties of Alloy T347 Foil," 2003, Allegheny Ludlum Technical Center internal report, Brackenridge, PA, available upon request.
28. Pint, B.A., and More, K.L., 2004 "Stainless Steels With Improved Oxidation Resistance for Recuperators," ASME paper GT2004-53627, Am. Soc. Mech. Engin., New York, NY.
29. Pint, B.A., Swindeman, R.W., More, K.L., and Tortorelli, P.F., 2001, "Materials Selection for High Temperature (750-1000°C) Metallic Recuperators for Improved Efficiency Microturbines," ASME paper 2001-GT-0445, Am. Soc. Mech. Engin., New York, NY.
30. Harper, M.A., Smith, G.D., Maziasz, P.J., and Swindeman, R.W., 2001, "Materials Selection for High Temperature Metal Recuperators," ASME paper 2001-GT-0540, Am. Soc. Mech. Engin., New York, NY.
31. Pint, B.A., More, K.L., and Tortorelli, P.F., 2002, "The Effect of Water Vapor on Oxidation Performance in Alloys Used In Recuperators," ASME paper GT-2002-30543, Am. Soc. Mech. Engin., New York, NY.
32. Maziasz, P.J., Pint, B.A., Swindeman, R.W., More, K.L., and Lara-Curzio, E., 2003, "Selection, Development and Testing of Stainless Steels and Alloys for High-Temperature Recuperator Applications," ASME paper GT-2003-38762, Am. Soc. Mech. Engin., New York, NY.
33. Swindeman, R.W., 1998, "Stainless Steels With Improved Strength for Service at 760°C and Above," PVP-Vol. 374, Fatigue, Environmental Factors and New Materials, Book No. H01155, Am. Soc. Mech. Engin., New York, NY, pp. 291-298.
34. Staubli, M., et al., "Materials for Advanced Steam Power Plants: The European COST522 Action," in Parsons 2003: Engineering Issues in Turbine Machinery, Power Plants and Renewables, The Institute of Materials, Minerals and Mining, Maney Publishing, London, U K, pp. 305-324.
35. Blum, R., and Vanstone, R.W., "Materials Development for Boilers and Steam Turbines Operating at 700°C," in Parsons 2003: Engineering Issues in Turbine Machinery, Power Plants and Renewables, The Institute of Materials, Minerals and Mining, Maney Publishing, London, UK, pp. 489-510.
36. Shingledecker, J.P., Swindeman, R.W., Klueh, R.L., and Maziasz, P.J., 2004, "Mechanical Properties and Analysis of Ultra-Supercritical Steam Boiler Materials," Proc. 29<sup>th</sup> International Technical Conference on Coal Utilization & Fuel Systems, National Energy Technology Laboratory, Morgantown, WV.
37. Kikuchi, M., Sakakibara, M., Otoguro, Y., Mimura, H., Araki, S., and Fujita, T., 1987, "An Austenitic Heat Resisting Steel Tube Developed For Advanced Fossil-Fired Steam Plants," in High Temperature Alloys, Their Exploitable Potential, Elsevier Science Publishing Co., New York, NY, pp. 267-276.
38. Takahashi, T., et al., 1988, "Development of High-Strength 20Cr-25Ni (NF709) Steel for USC Boiler Tubes," Nippon Steel Technical Report No. 38 (July 1988), Nippon Steel Corp., Tokyo, Japan.
39. Quality and Properties of NF709 Austenitic Stainless Steel for Boiler Turbing Applications, 1996, Nippon Steel Corp., Revision 1.1, Tokyo, Japan.
40. Lara-Curzio, E., Maziasz, P.J., Pint, B.A., Stewart, M., Hamrin, D., Lipovich, N., and DeMore, D., 2002, "Test Facility for Screening and Evaluating Candidate Materials for Advanced Microturbine Recuperators," ASME paper GT-2002-30581, Am. Soc. Mech. Engin., New York, NY.
41. Lara-Curzio, E., Trejo, R., More, K.L., Maziasz, P.J., and Pint, B.A., 2005, "Evaluation and Characterization of Iron- and Nickel-Based Alloys for Microturbine Recuperators," ASME paper GT2005-68630, Am. Soc. Mech. Engin., New York, NY.

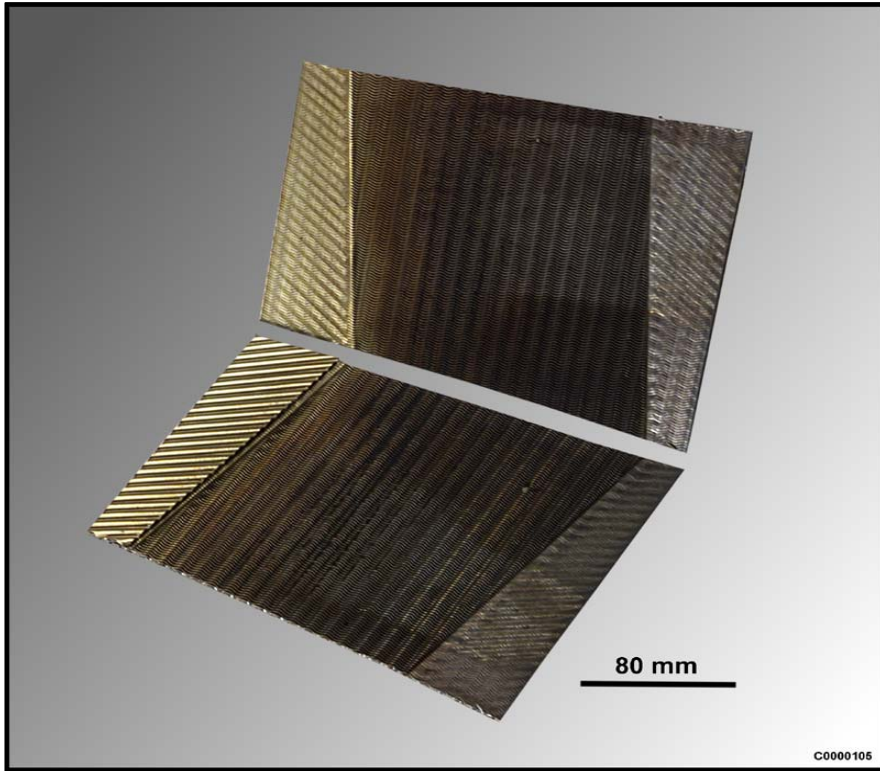
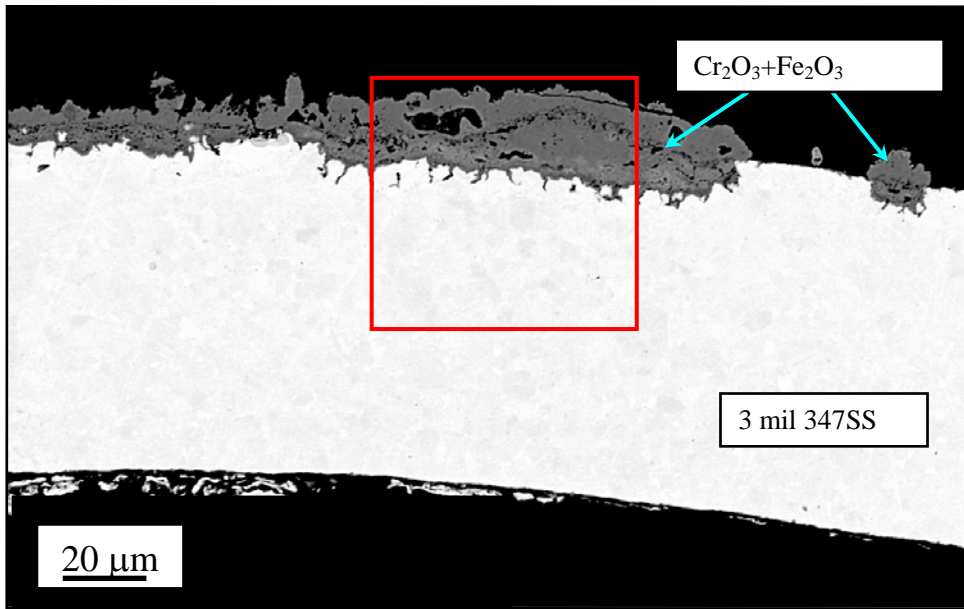
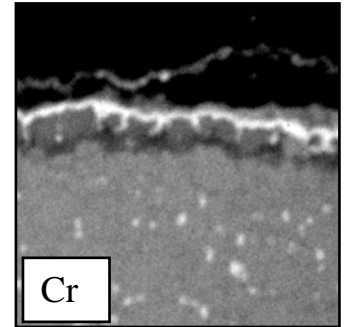


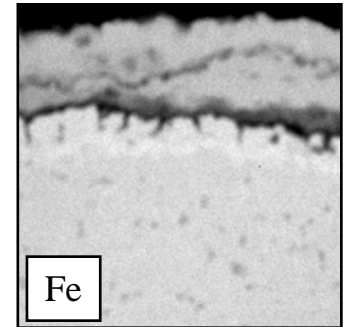
Figure 1 – Photograph of two PSR aircells from a Honeywell recuperator made from 347 stainless steel foil, after relatively short term microturbine exposure. The darker right-hand portion of the air cell has seen the maximum temperature and oxidation, whereas the lighter golden left-hand side has seen a lower temperature and has developed a slight heat tint; this indicates the temperature gradient across the air cell that such components typically have due to the counterflows of cool air and hot exhaust. This component showed no evident of AA yet.



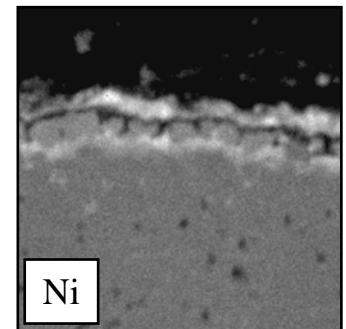
b



c



d



a

Figure 2 – a) Scanning electron microscope (SEM) back-scattered electron (BSE) imaging of 347 stainless steel air-cell foil cross-section from a recuperator with significant service in a microturbine. It shows (a) the formation of heavy, Fe-rich oxide nodules at the exhaust-side surface (higher % of H<sub>2</sub>O) that are characteristic of the onset of AA due to oxidation in the presence of water vapor. Higher magnification SEM X-ray mapping images using K $\alpha$  peaks of the elements indicated show the complex nature of the surface oxides for the elements (b) Cr, (c) Fe, and (d) Ni. The thick outer oxide scale is Fe-rich (c), with a thin Cr-rich oxide (b) and a Ni-depleted region in the sub-surface metal beneath (d).

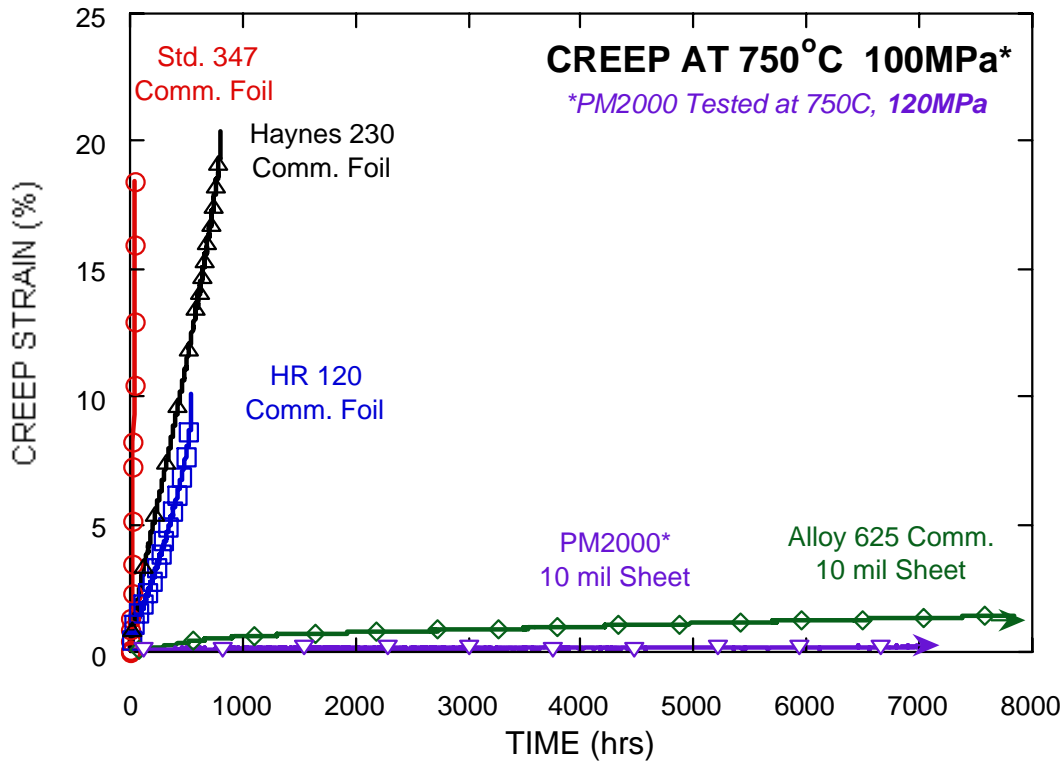


Fig. 3, Creep data for commercial sheets and foils tested at 750°C and 100 MPa (except for the PM2000 ODS alloy, tested at 120 MPa) in air. The 3-4 mil (0.003-0.004 inch thick) foils crept at a high rate with little secondary creep regime, but both the HR120 and HR230 alloy foils exhibited almost 10 times longer rupture life than typical 347 steel foil. By contrast, both alloy 625 and the PM2000 (ODS ferritic alloy) exhibited a prolonged secondary creep regime, with a very low creep rate, and lasted more than 100 times longer than 347 steel (still in test).

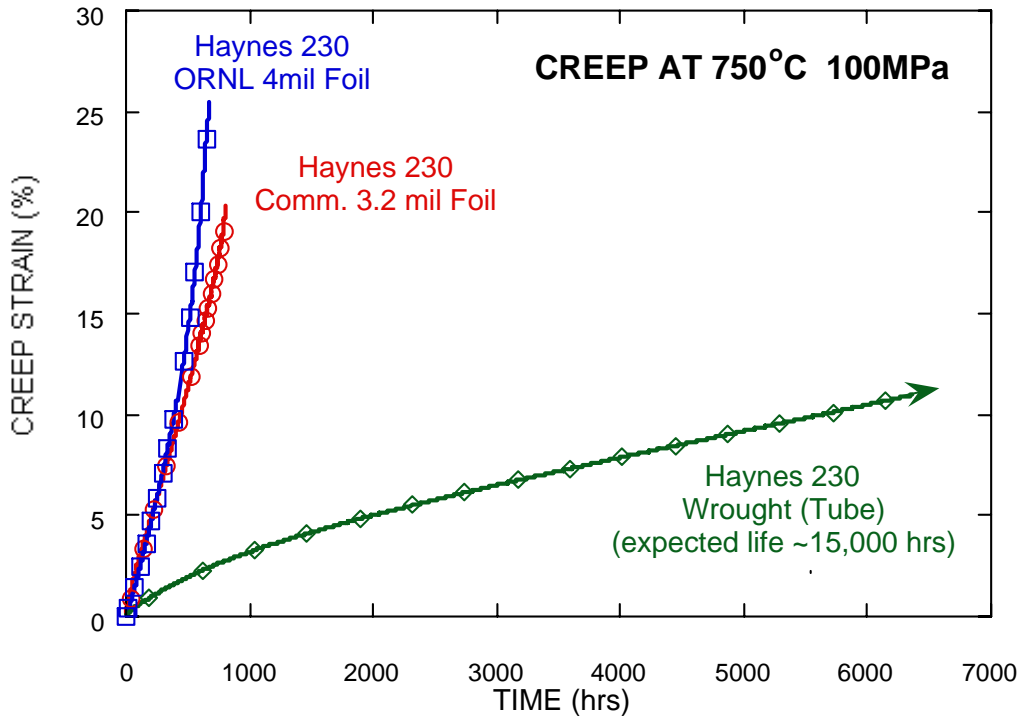


Fig. 4 – Creep tests of fine-grained foils and coarser-grained tubing of HR230, illustrating the fine-grain size effect, which dramatically reduced or eliminated the secondary creep regime, when that grain size was below the critical grain size for creep resistance. Such data are the basis for the premise that foil behavior cannot be predicted from creep data on tube or plate of the same alloy.

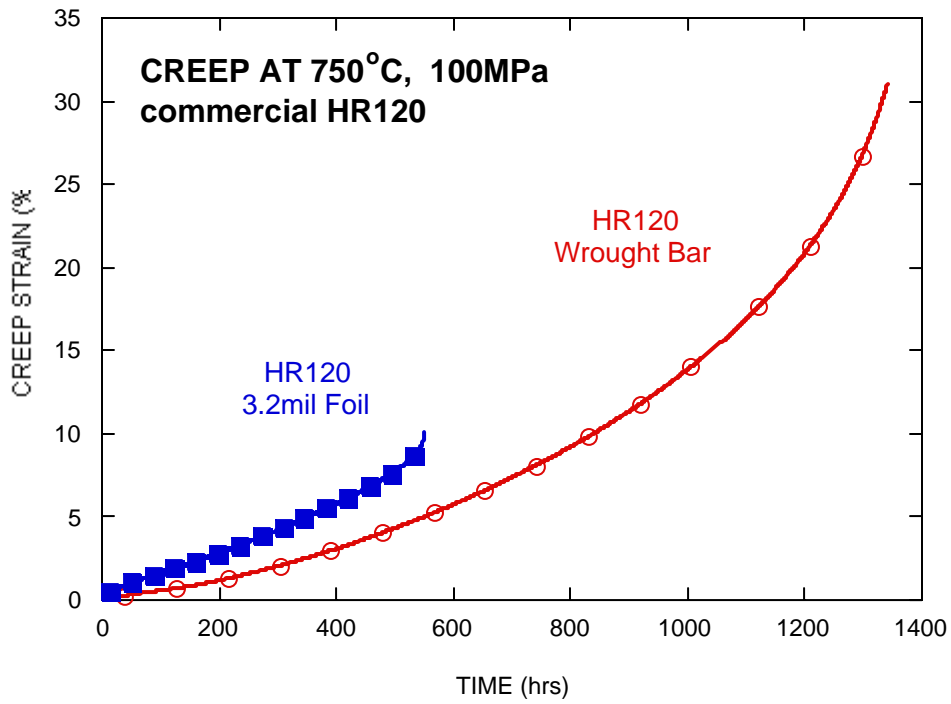


Fig. 5 - Creep testing of foil and bar of alloy HR 120 shows roughly parallel creep curves, despite significant differences in processing and grain size between these specimens.

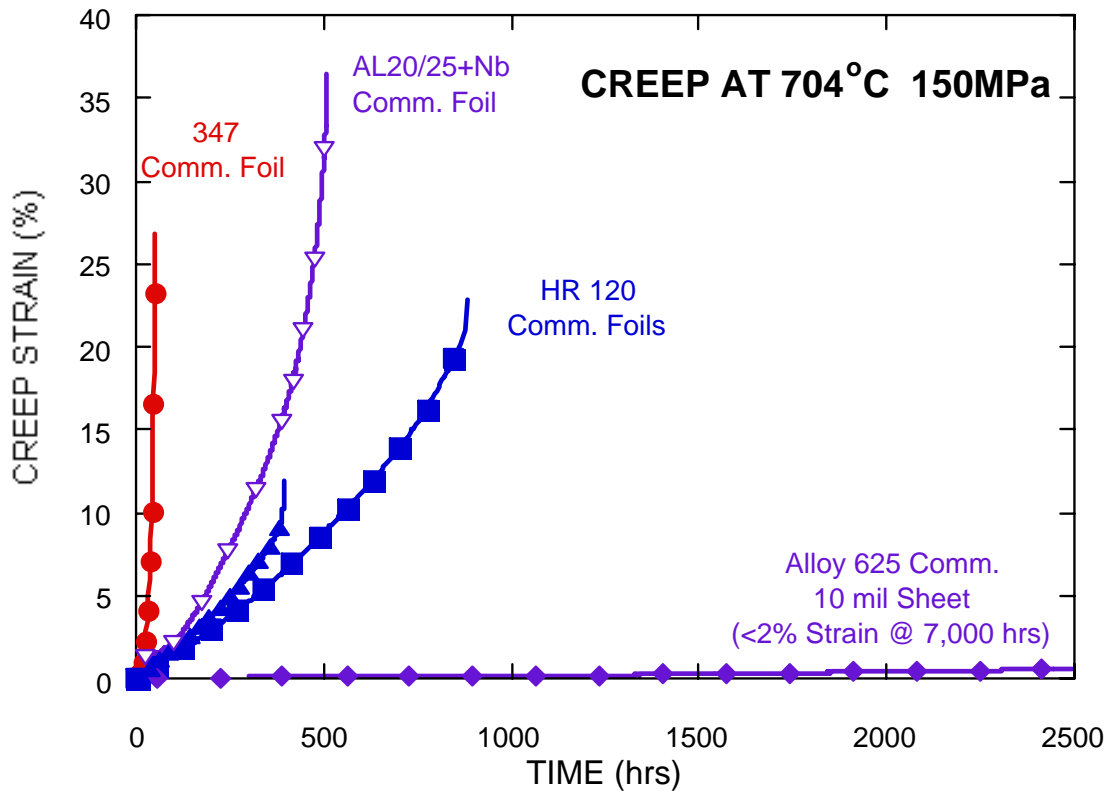


Fig. 6 - Creep data on commercial sheets and foils tested at 704°C and 150 MPa in air. Two different foils of HR120 showed similar creep curves, but differences in rupture elongation that directly determine the differences in rupture lifetime. Foil of the new AL20-25+Nb alloy showed a slightly higher creep rate than HR120, but both were many times better than 347 steel. Sheet of alloy 625 showed little or no creep at these conditions.

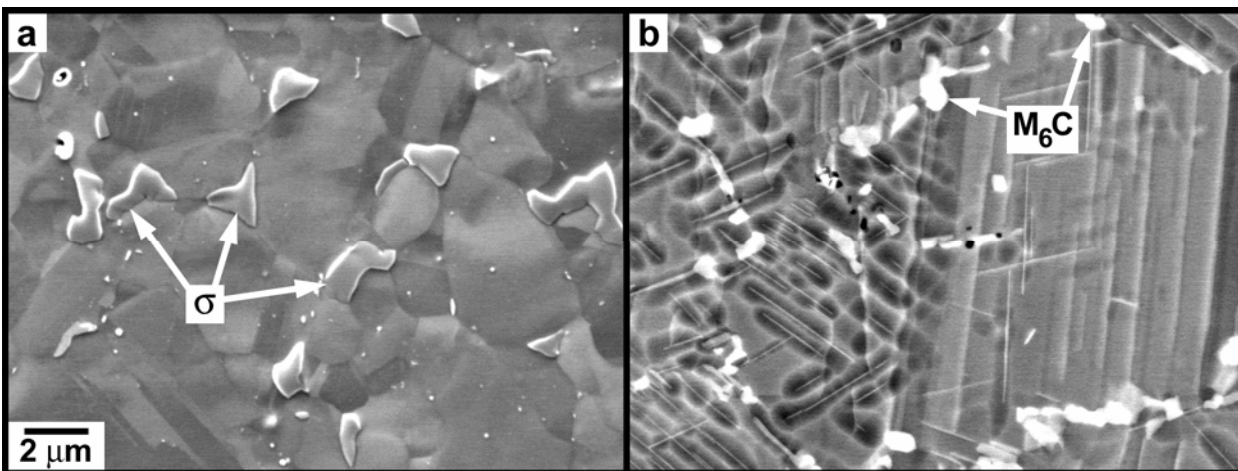


Fig. 7 – SEM micrographs showed a) formation of Fe-Cr  $\sigma$ -phase at grain boundaries in 347 steel during creep at 704°C and 152 MPa (rupture after only 51.4 h), whereas b) a relatively stable dispersion of Si-Mo-Cr-Ni  $M_6C$  phase developed and remained stable along grain boundaries of alloy 625 during creep at 750°C and 100 MPa (rupture after 4510 h).

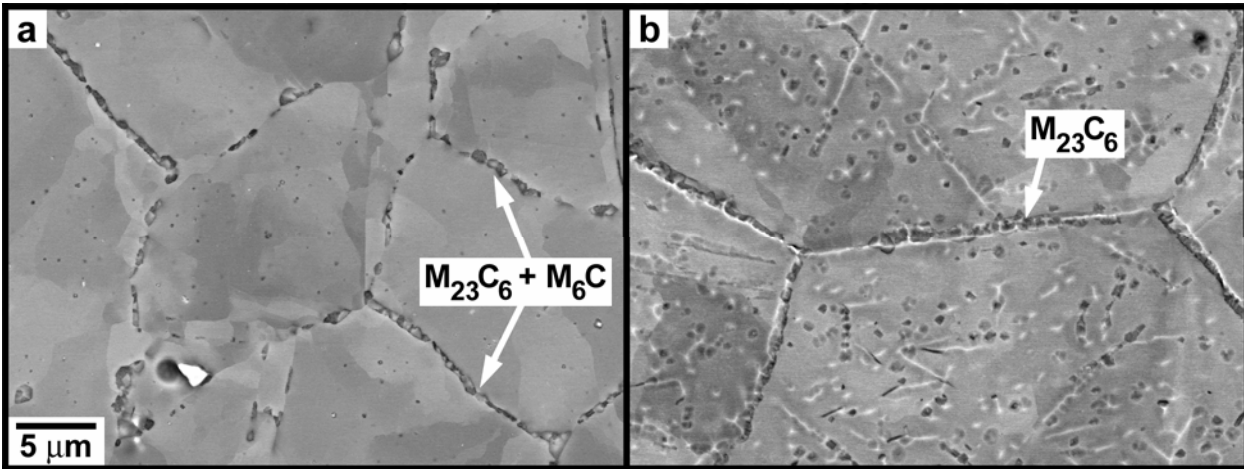


Fig. 8 – SEM micrographs show the precipitation that occurred along grain boundaries in foils of a) alloy NF709 (rupture after 5015h), and b) alloy HR120 (rupture after 3319h), both creep tested at 750°C and 100 MPa. The NF709 alloy has mainly the Si-Mo-Cr-Ni M<sub>6</sub>C particles with some Cr-rich M<sub>23</sub>C<sub>6</sub> particles, while the HR120 alloy has only M<sub>23</sub>C<sub>6</sub> particles dispersed along the grain boundaries and in the matrix.

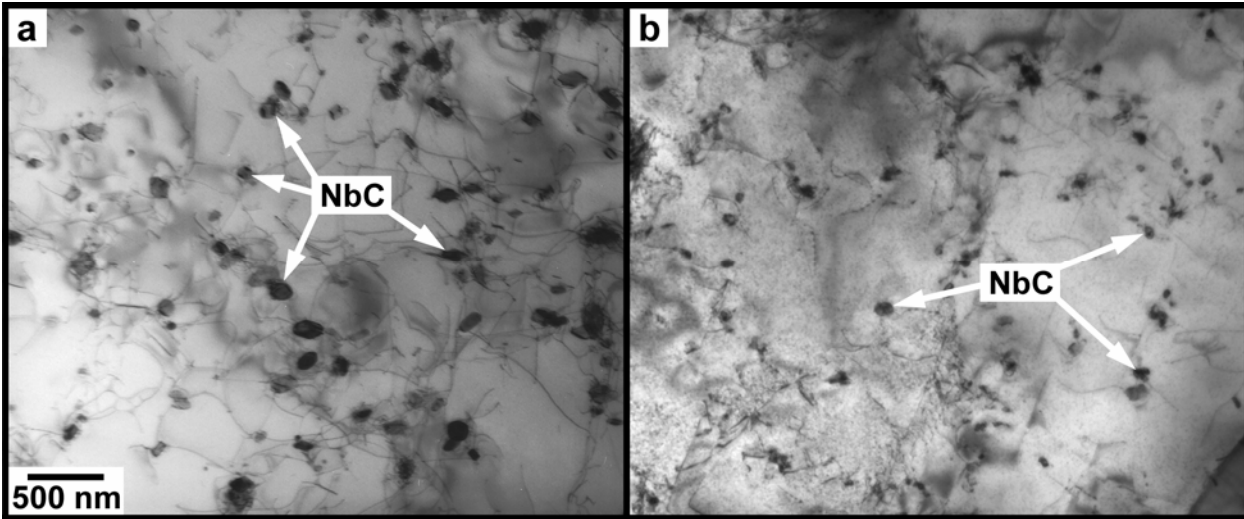


Fig. 9 – TEM micrographs show the fine NbC precipitation within the grains in foils of a) alloy NF709 (rupture after 5015h), and b) alloy HR120 (rupture after 3319h), both creep tested at 750°C and 100 MPa.